PAPER ID: 1144
DOI: 10.18462/iir.rankine.2020.1144

Dynamic Analysis of Energy Recovery Utilizing Thermal Storage from Batch-Wise Metal Casting

Trond ANDRESEN[(a,*)], Simon LINGAAS[(b)], Brede A. L. HAGEN[(b)], Petter NEKSÅ[(a)]

[(a)] SINTEF Energy Research,
Trondheim, 7034, Norway, [*]trond.andresen@sintef.no
[(b)] Norwegian University of Science and Technology (NTNU), Trondheim, 7034, Norway

ABSTRACT

The thermal exergy contained in the liquid metal in ferroalloy production makes it an interesting source for energy recovery. The heat released during casting is rarely utilized today. This work investigates the feasibility of continuous power production from batch wise ferroalloy casting using an energy recovery system concept that includes a thermal energy storage to buffer captured heat between casting cycles and enable a more stable heat supply to a Rankine cycle. A dynamic model of the heat recovery and storage system was developed, and a demonstration case applied to evaluate basic system behaviour. Every two hours, liquid metal at 1450 °C was poured into moulds and placed in a cooling tunnel. With the investigated concept, only 54.6 % of the available heat was captured into the system, indicating a potential for further improvements. Overall, the system was able to output 667 kWh_{el} from the 4 005 kWh of thermal exergy available in the metal in each casting cycle, equivalent to an exergy efficiency of 16.7 %.

Keywords: Waste heat recovery, Intermittent heat source, Dynamic analysis, Rankine cycle, Energy storage.

1. INTRODUCTION

In order to reduce greenhouse gas emissions and lessen the effects of climate change, it is vital to improve upon the energy efficiency in the industry. One way to increase the industrial energy efficiency is waste heat recovery. The metal industry has large potential for waste heat recovery. The waste heat recovery potential from the iron and steel industry in EU is estimated to be 72 TWh/year (Vance et al., 2019). Off-gases contain the major part of the waste heat in the metal industry. However, the high temperature heat that is released during metal casting has higher specific exergy content and is consequently interesting to consider as a heat source for power production. The casting processes in many steel plants, and all Norwegian ferroalloy and silicon plants (Tangstad, 2013), are performed batch-wise. This adds complexity to both heat capture and practical power production. Due to the high initial temperatures of the metal during casting, radiation is likely the dominant mechanism for heat loss. As radiative power is proportional to the surface temperature to the power of 4, there will be significant and non-linear variations in radiative heat dissipation during a casting cycle. The time from casting until full solidification is also a matter of importance, as it can negatively affect mechanical strength and distribution of impurities in the final product if solidification occurs too quickly or too slowly (Tveit, 1988). A heat recovery system aiming for high utilization rate of heat from metal casting should be designed to handle considerable fluctuations in heat input, as well as being able to buffer captured heat to enable continuous heat and/or power output between batches.

Several concepts for recovering heat released during casting has been proposed in the literature. A flat heat pipe recovery system was designed to recover radiant heat in the steel production industry (Jouhara et al., 2017). A pilot system was built and implemented on a steel wire cooling process, and reported to recover 700 kW of heat. The feasibility of other radiative heat sources has also been examined, such as the ceramics industry (Delpech et al., 2019) or from rotary kilns (Caputo et al., 2011; Du et al., 2018).

In this work we explore the hypothetical feasibility of a proposed integrated power production system aiming to achieve high utilization and conversion efficiency of the available thermal energy in the hot liquid metal, while featuring options for controlling desired cooling rates and continuous power production despite the

intermittent nature of batch casting. The proposed system solution consists of a Heat Recovery Heat Exchanger (HRHE) extracting heat from the liquid metal, a Thermal Energy Storage (TES) for smoothing the time-variability of the heat source and a heat transfer fluid loop supplying heat to a Rankine cycle. Analysing the thermal behaviour of the thermal input and heat recovery system as a crucial first step towards enabling practical and efficient power production from such heat sources. Main focus in this work is thus the feasibility of capturing and translating intermittent heat input from casted metal into sufficiently smooth heat supply to a Rankine cycle, while the Rankine cycle itself is represented quite simplified. The paper is organised as follows: Section 2 presents the proposed power production system. Section 3 presents the methodology used for modelling and simulation of the power production system. The case study used for demonstrating the proposed power production system is presented in Section 4. Section 5 presents and discusses results from the case study. The conclusions drawn from this study are presented in Section 6.

2. ENERGY RECOVERY CONCEPT

Aiming to achieve high power output and controllable metal cooling rates, a system concept for power production is proposed, see Figure 1. A metal production plant with batchwise casting is used as basis for these considerations. The main sequence of each cycle with the proposed system, as shown in Figure 1, is: 1) Molten metal is sequentially poured into moulds, which are moved into a cooling tunnel when full. 2) The moulds stay inside the tunnel for a period of time while dissipating heat to both the ambient and a heat exchanger. 3) The tunnel is emptied and prepared for a new cycle. The extracted moulds can be cooled further with e.g. direct water spray as necessary before being processed further.

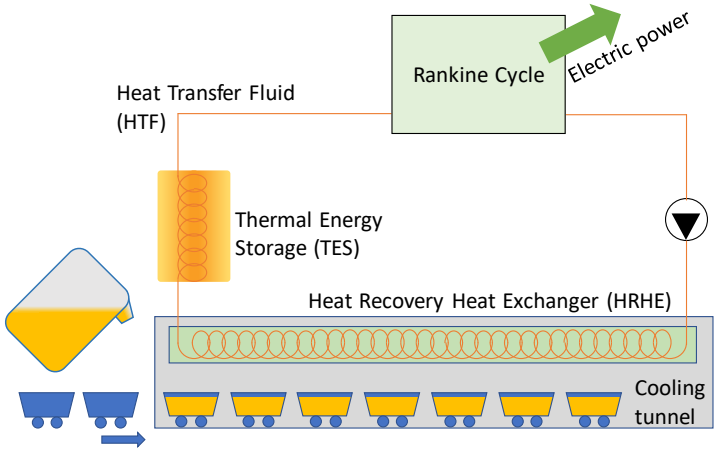

Figure 1: Simple system concept diagram

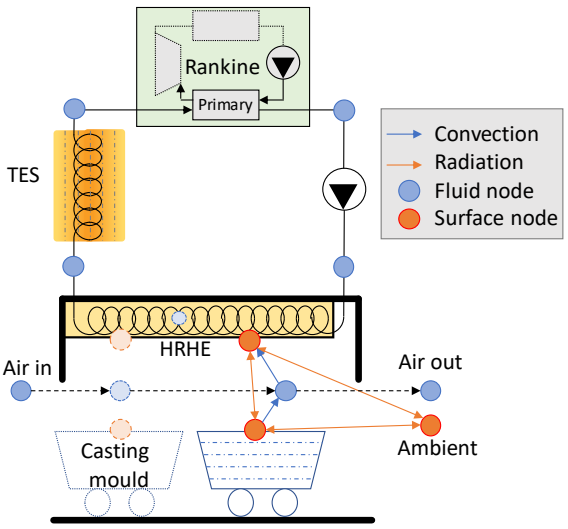

Figure 2: System modelling principles

Inside the cooling tunnel, a heat recovery heat exchanger (HRHE) absorbs heat from the cooling metal and transfers it to the heat transfer fluid (HTF). From the HRHE, the HTF is circulated through a thermal energy storage (TES) and further on to the Rankine cycle's evaporator. The TES will buffer thermal energy to supply the Rankine cycle in the periods without (sufficient) heat input to the HRHE, as well as help mitigate rapid fluctuations in heat input. The temperature level of the HTF loop and TES during a cycle is possible to control through both system design and variables such as fluid flow rates. However, identifying optimum temperatures in dynamic systems such as this is not trivial. Heat-to-power conversion has a higher theoretical maximum efficiency with increasing temperature. At the same time, the temperature level in the TES, HTF loop, and HRHE will determine how much of the thermal energy in the heat source that can be recovered. Higher temperatures in the HTF loop allows for less utilization of the heat source, as heat cannot be recovered when the source is cooled down below the temperature of the fluid in the HRHE.

The proposed system utilizes a single HTF loop for both charging and discharging of the thermal energy storage, instead of having separate loops for charging and discharging. Such systems enable active control of charging and discharging, for example with use of temperature set points in the TES or HTF loop. A single loop system simplifies modeling and operation and does not require a controller to operate the system.

3. METHODOLOGY

A dynamic model of the energy recovery system was implemented using the programming language Modelica, with Dymola being used as the platform for modelling and simulation. The basic modelling principles and included mechanisms of the component models is described in the remainder of this section. The reader is referred to Lingaas (2019) for details regarding governing equations and model code, as well as validation of the individual submodels using reported measurements from the literature. Models for the cooling tunnel, HRHE, and TES were based on geometry parameters such as basic overall dimensions and channel diameters for fluid flow. This enables the use of the overall system model to explore effects of individual component sizes and configurations. Fluid flow was modelled with constant fluid properties and using control volumes. Convective heat transfer coefficients were calculated with the Gnielinski (2013) correlation.

3.1. Cooling tunnel with Heat Recovery Heat Exchanger

Figure 2 illustrates the basic model principles for the cooling tunnel and HTF loop. The cooling tunnel includes several casting moulds, the heat recovery heat exchanger, tunnel wall, and air flow. The sub-models are discretized along the length of the tunnel. The HRHE is modelled as heat transfer surfaces coupled on one side to the tunnel air and to the HTF on the other. The HRHE surface area facing the air equals the tunnel footprint. Heat loss from the HRHE to the ambient via the tunnel walls is calculated using a constant heat transfer coefficient. Convective heat transfer is modelled between the air and HRHE outer surface, HTF and HRHE inner surface, and the air and the casting mould surface. Radiative heat transfer is modelled using the radiation heat transfer network method described in (Incorpera et al., 2006). Three surfaces are considered here: the surface of the casted metal, the HRHE outer surface, and the surroundings, i.e. radiation lost through the tunnel openings in each end. The surroundings are assumed to be a black body with emissivity of 1 from which insignificant amounts of heat radiate back into the tunnel. A fixed flow rate of air through the tunnel is assumed.

3.2. Casting mould

Each casting mould is modelled as a box-shaped thermal mass discretized both vertically and along the tunnel length axis. The mould model only considers the casted metal, ignoring any physical and thermal impact of a mould frame itself. The mould has one external surface facing upwards exchanging heat with the surroundings, and the other surfaces are assumed to be adiabatic. This is similar to other simple metal solidification models (Benham et al., 2016). The sum of mould surface areas is equal to the tunnel footprint (length x width). For a fixed mass of metal, the specified tunnel footprint thus also determines the exposed mould surface area and the mould depth. Mould surface area directly influences radiative power. Heat conduction between each layer is modelled using thermal resistances. Temperature dependent enthalpy reflects both a constant heat capacity and the enthalpy of fusion in the liquidus-solidus temperature interval. For the material used in the demonstration case described in Section 4, the heat capacity was 0.812 $kJ \times kg^{-1} \times K^{-1}$ for both liquid and solid phases, and the enthalpy of fusion was 1100 $kJ \times kg^{-1}$ uniformly distributed over the interval of 1350 - 1205 °C.

3.3. Thermal energy storage

The thermal energy storage (TES) was modelled as described by Jian (2015), where a thermal energy storage is modelled using the lumped capacitance assumption while defining an effective heat transfer coefficient to describe heat transfer from the HTF to the storage material. To simplify the model, a single heat transfer tube with its surrounding material was modelled, and the model was scaled up assuming symmetry to properly represent the actual size of the storage. Constant thermal properties of the storage material were assumed.

3.4. Rankine cycle

As the primary focus in this work is behaviour and performance of the overall heat capture system, the Rankine cycle is represented in a quite simplified manner. Only the behaviour of the HTF exchanging heat with the working fluid (WF) in the primary heat exchanger is considered. The primary heat exchanger is discretized into several control volumes of equal and constant UA-value. The working fluid enters the primary heat exchanger at a fixed temperature and flow rate, and the outlet temperature is calculated based on the heat transferred. Net power produced, $\dot{W}_{el}$, is estimated using a fixed exergy efficiency, B, multiplied with the exergy transferred *into* the Rankine cycle; $\dot{W}_{el} = B * \eta_{carnot} * \dot{Q}_{Primary}$, where $\eta_{carnot} = 1 - \frac{T_{amb}}{T_{HTF,in} - T_{HTF,out}} * ln\left(\frac{T_{HTF,in}}{T_{HTF,out}}\right)$. In other words, the working fluid side of the Rankine cycle is not directly used

to estimate net power. However, the load- and temperature variable behaviour in this heat exchanger affects heat transfer and temperatures in the rest of the HTF loop. This modelling principle, though simplified, provides an estimate for net power sensitive to input exergy as well as realistic impact on the HTF loop. With a constant *B*, part load characteristics are disregarded. We believe this simplification to be adequate, because the intention is to explore the overall system feasibility for integration of a generic power cycle, and not for accurate performance prediction of a specific Rankine cycle.

4. DEMONSTRATION CASE

The model is demonstrated on a test case representing a hypothetical silicon furnace based on parameters and conditions described in Børset (2015); every two hours, 9000 kg of liquid Silicon at 1450°C is cast into multiple moulds and allowed to cool down. A measuring campaign indicated that complete solidification of a mould was reached in 36 minutes after casting, which would be a target to match also in the current work.

The system model was set up using the parameters listed in Table 1. Superheated steam at 20 bar was considered as HTF, and concrete as the TES material. The specified TES thermal capacity of 50 $MJ \times K^{-1}$ is equivalent to 13.7 m^3 of concrete. The parameter *tunnel* height is used as the distance from the top of the mould to the surface of the HRHE. The model was initialized by running the model for several cycles until reaching a cyclic steady state. The system was operated without controllers to govern HTF and WF flow rates, thus relying on the behaviour of the system design to mitigate the variability in heat input. The demonstration case results should therefore be considered as conservative regarding any estimates for energy recovery potential.

Table 1: Key model parameters used in demonstration case

Property	Unit	Value	Property	Unit	Value
General			***Tunnel***		
Ambient temperature	°C	25	Dimensions L x W x H	m	21.8 x 2 x 1
Casting cycle duration	s	7 200	Tunnel segments	-	30
Time to fill all moulds	s	1 800	Wall insulation thickness	m	0.01
Mould time inside tunnel	s	6 480	Insulation conductivity	$W \times m^{-1} \times K^{-1}$	0.055
Silicon mass per cycle	kg	9 000	Air flow velocity	$m \times s^{-1}$	1
Silicon initial temperature	°C	1 450	HRHE channel diameter	m	0.1
Silicon emissivity	-	0.55	HRHE surface emissivity	-	0.8
Number of moulds	-	10	***Thermal energy storage***		
Mould vertical segments	-	15	Density	$kg \times m^{-3}$	3 100
Rankine exergy efficiency, *B*	-	50 %	Specific heat capacity	$J \times kg^{-1} \times K^{-1}$	1 100
Heat Transfer Fluid (HTF)	-	Steam	Thermal conductivity	$W \times m^{-1} \times K^{-1}$	2.65
HTF pressure	bar	20	Total thermal capacity	$MJ \times K^{-1}$	50
HTF mass flow rate	$kg \times s^{-1}$	15	Channel diameter	m	0.15
			Channel pitch	m	0.9

5. RESULTS AND DISCUSSION

Summarized results from one casting cycle are shown in Table 2. The system managed to fully solidify the silicon within the targeted 36 minutes. Figure 3 shows the temperature distribution in one casting mould for the duration of the casting cycle. At the end of the cycle, the moulds exited the cooling tunnel at an average temperature of 427 °C. At this point, the metal contained around 15% of the initial thermal energy but only 8 % of the initial thermal exergy. The potential for further energy recovery is therefore quite limited. Overall, the system managed to recover 54.6% of the thermal energy, and 16.7% of the thermal exergy initially present in the molten metal. For 8000 hours of operation annually, the system could produce 2.7 GWh_{el}/y. Figure 4 shows the overall heat flows surrounding the tunnel, including losses to the ambient via different paths. The

Published with the authorization of the International Institute of Refrigeration (IIR).
The conference proceedings of the IIR Rankine Conference 2020 are available in the Fridoc database on the IIR website at www.iifiir.org

10 sharp spikes in heat flow indicate the introduction of each mould into the tunnel. The rapid initial decline after each spike is the result of the metal surface cooling down to the onset of solidification within a couple of minutes. The surface cooling from the initial 1450 °C to 1350 °C reduces the radiative heat loss by over 20%.

Table 2: Summarized results from simulation

Property	Unit	Value
Initial thermal energy in Si	MWh	5.64
Initial thermal exergy in Si	MWh	4.05
Thermal energy recovered in the HRHE	MWh	3.08
Electric energy produced	kWh_{el}	676
Maximum variation in power output	kW_{el}	259
Average metal temperature at cycle end	°C	427
Remaining thermal energy in Si at cycle end	MWh	0.81
Remaining thermal exergy in Si at cycle end	MWh	0.25
Metal solidification time	min	36
Average TES temperature	°C	384
Maximum local TES temperature	°C	427
Variation in WF turbine inlet temperature	K	106

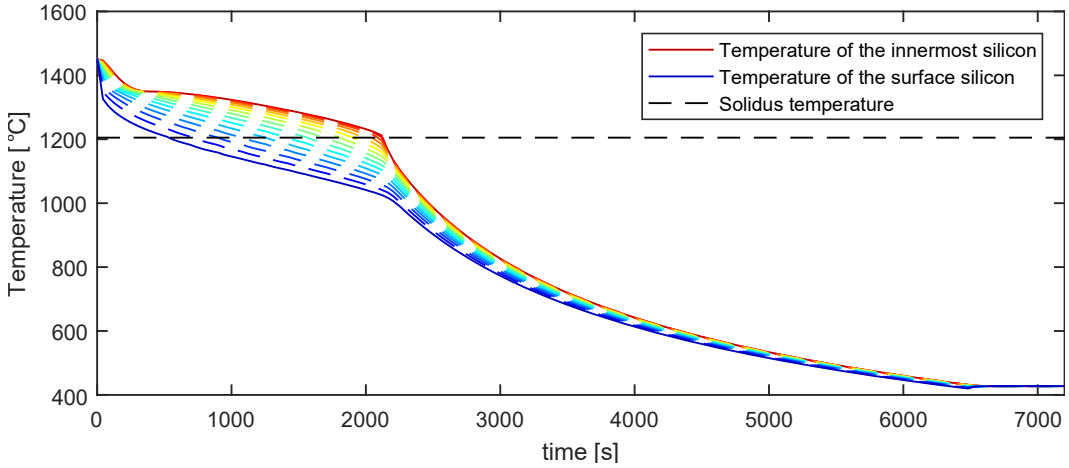

Figure 3: Temperature distribution in one casting mould

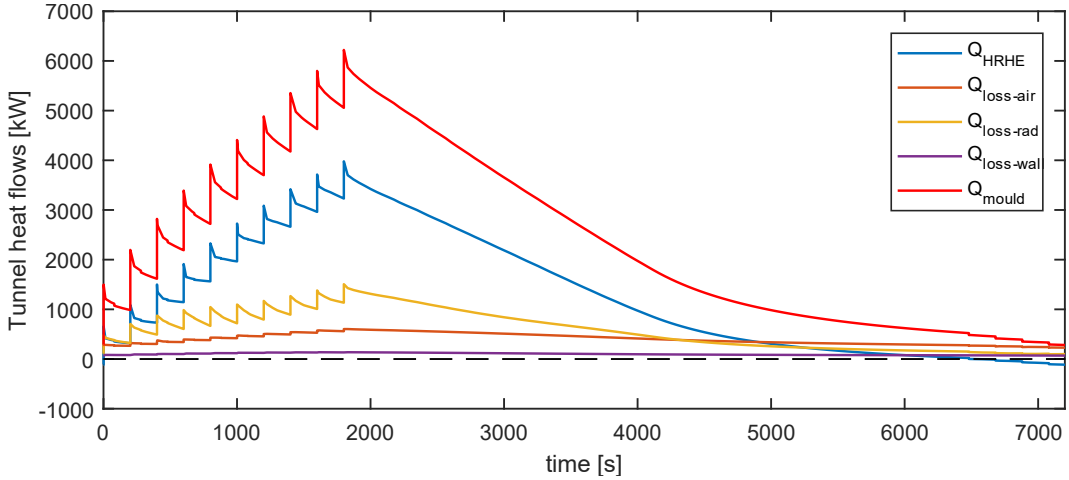

Figure 4: Heat flows around the cooling tunnel

The largest heat loss is caused by radiation through the openings in each end of the tunnel. Convective heat loss to the air flow is also significant. Both losses could likely be reduced by changing the tunnel geometry to reduce radiation paths to the ambient or by adding doors to fully close the tunnel during operation.

Additional heat flows and temperature profiles are shown in Figure 5 a-d. The average HRHE heat flow was 1.54 MW, with a peak of 4 MW. Given the constraint on solidification time, this peak cannot be easily reduced by for example controlling the heat dissipation rate. The system output was 338 kW_{el} electric power on average, but with a variation between maximum and minimum power output of 260 kW_{el} as can be seen by the W_{net} line in Figure 5a. However, the system managed a fairly consistent power output considering the much larger variation in heat and exergy input, and the lack of active control of both heat buffering and Rankine cycle. Unlike the large variations in HRHE duty, it should be feasible to reduce variations in Rankine power output by implementing control strategies and considering more advanced system configurations the allow better control of heat flow from the HTF loop to the TES and Rankine cycle.

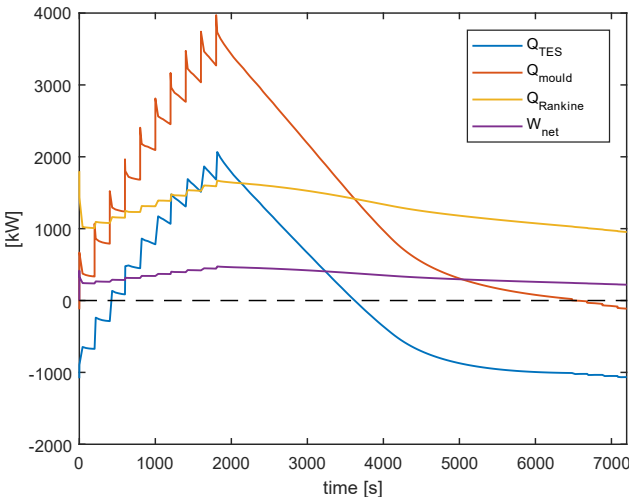

a) Key heat flows and net power

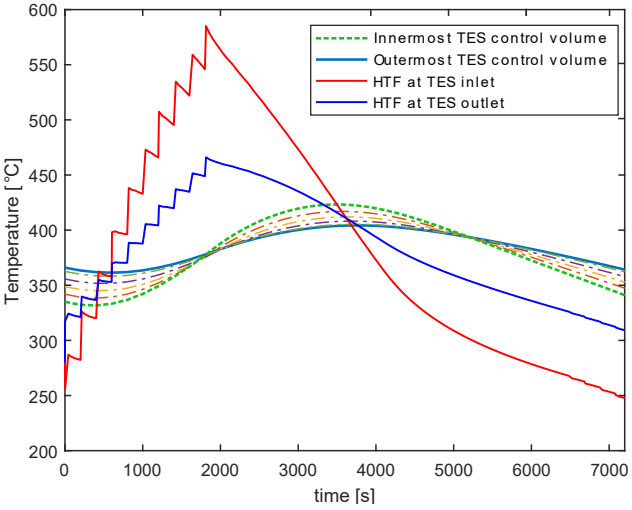

b) Temperature profiles in the TES

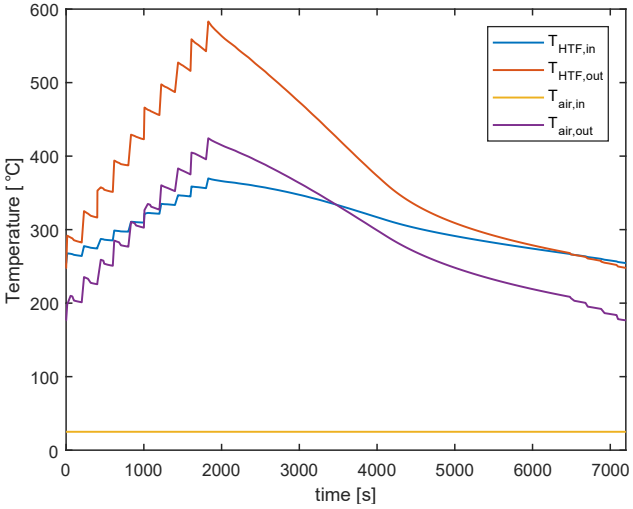

c) Air and HTF temperatures at inlet and outlet of cooling tunnel

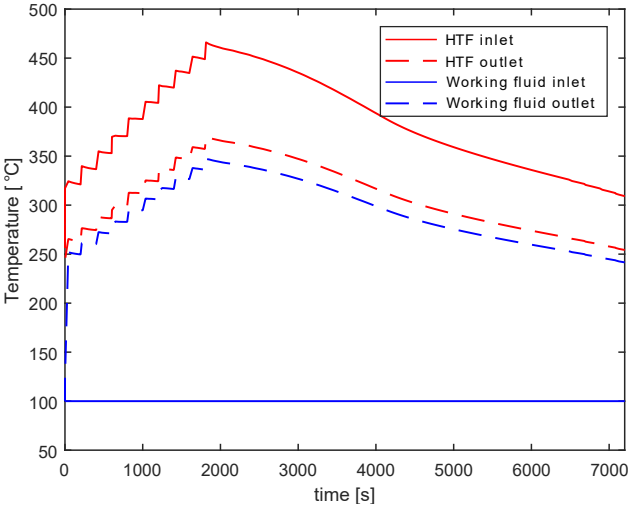

d) HTF and WF temperatures in and out of the Rankine cycle primary heat exchanger

Figure 5: Heat flows and temperature profiles

The effect of the TES in the system can also be analysed in Figure 5. In Figure 5a, the blue line represents TES heat input. From ~500 to ~3500 seconds into the cycle, TES heat input is above zero, indicating that the TES is being charged. The rest of the time, the TES provides a net heat input to the HTF loop. Figure 5b shows temperatures of the thermal storage control volumes and the HFT in the TES. The average TES temperature was 384 °C, with variations during the cycle of ±50 K. Figure 5d shows fluid temperatures across the primary heat exchanger in the Rankine cycle. As discussed in Chapter 3, only the HFT side was used to estimate power production potential. The average HTF inlet temperature at the Rankine primary heat exchanger was around

Published with the authorization of the International Institute of Refrigeration (IIR).
The conference proceedings of the IIR Rankine Conference 2020 are available in the Fridoc database on the IIR website at www.iifiir.org

350 °C, indicating that much of the specific exergy from the heat source was lost even before reaching the Rankine cycle. At least parts of these losses are intrinsic to the cyclic availability of the heat source in the explored case.

Figure 6 illustrates the impact of a TES in the system. The system was simulated again with identical parameters but with the TES removed. Without any TES, the system experiences a fluctuation in HTF temperature at the HRHE outlet of 425 K, compared to around 100 K with the specified thermal capacity in the demonstration case.

Figure 7 shows the distribution of heat loss from the silicon moulds accumulated over one casting cycle for different tunnel heights. With all other parameters fixed, simulation results for different tunnel heights shows a significant potential to improve fraction of heat recovered in the HRHE.

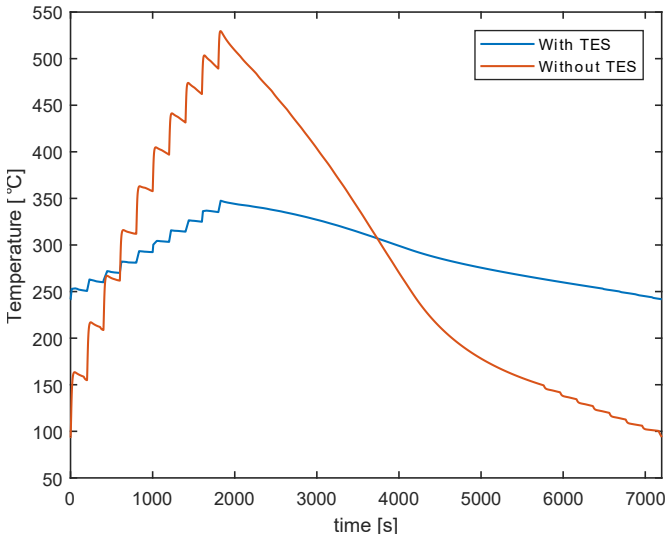

Figure 6: HRHE HTF outlet temperature with and without TES present in system

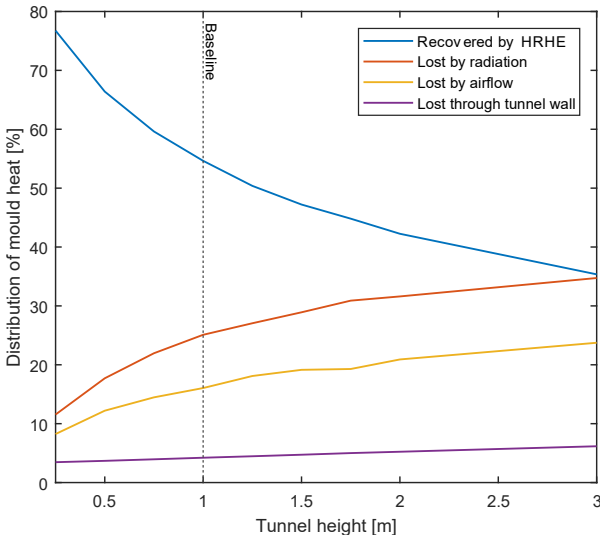

Figure 7: Overall mould heat loss distribution at varying tunnel height

6. CONCLUSIONS

This work has investigated the feasibility of continuous heat recovery and power production from batch wise metal casting. An energy recovery system concept was described, and a dynamic model developed. A demonstration case was applied to evaluate basic system behaviour and to provide some insight into practical feasibility. The simulation results indicated that the heat recovery heat exchanger and heat transfer loop must handle significant variations in heat load, but even the fairly simple thermal energy storage configuration analysed in this work was found to buffer heat input fluctuations well. Overall, the system was able to output 667 kWh_{el} from the 4 005 kWh of exergy available in the metal each casting cycle, equivalent to an exergy efficiency of 16.7 %. However, only 54.6 % of the available heat was captured into the system, indicating a potential for design and control improvements. The dynamic system model proved capable of providing useful insights into the behaviour of such an energy recovery system. Future work should expand the model to consider a full Rankine cycle to enable more accurate power conversion estimates, evaluate control strategies, and analysis of practical feasibility.

ACKNOWLEDGEMENTS

This publication has been funded by HighEFF - Centre for an Energy Efficient and Competitive Industry for the Future, an 8-year Research Centre under the FME-scheme (Centre for Environment-friendly Energy Research, 257632). The authors gratefully acknowledge the financial support from the Research Council of Norway and user partners of HighEFF.

REFERENCES

Benham, G., Hildal, K., Please, C. P., Van Gorder, R. A., 2016. Solidification of silicon in a one-dimensional slab and a two-dimensional wedge. International Journal of Heat and Mass Transfer 98, 530-540.

Børset, M. T., 2015. Energy Dissipation and Recovery in the Context of Silicon Production: Exergy Analysis and Thermoelectricity. PhD thesis, Norwegian University of Science and Technology.

Caputo, A. C., Pelagagge, P. M., Salini, P., 2011. Performance modeling of radiant heat recovery exchangers for rotary kilns. Applied Thermal Engineering 31(14-15), 2578-2589.

Delpech, B., Axcell, B., Jouhara, H., 2019. Experimental investigation of a radiative heat pipe for waste heat recovery in a ceramics kiln. Energy 170, 636 – 651.

Du, W. J., Yin, Q., Cheng, L., 2018. Experiments on novel heat recovery systems on rotary kilns. Applied Thermal Engineering 139, 535 – 541.

Gnielinski, V., 2013. On heat transfer in tubes, Int. J. of Heat and Mass Transfer 63, 134-140.

Incorpera, F. P., Dewitt, D. P., Bermann, T. L., Lavine, A. S., 2005. Fundamentals of Heat and Mass Transfer, 6th ed. John Wiley & Sons, 2005.

Jian, Y., Bai, F., Falcoz, Q., Xu, C., Wang, Y., Wang, Z., 2015, Thermal analysis and design of solid energy storage systems using a modified lumped capacitance method. Applied Thermal Engineering 75, 213 – 223.

Jouhara, H., Almahmoud, S., Chauhan, A., Delpech, B., Bianchi, G., Tassou, S. A., Llera, R., Lago, F., Arribas, J. J., 2017. Experimental and theoretical investigation of a flat heat pipe heat exchanger for waste heat recovery in the steel industry. Energy 141, 1928-1939.

Lingaas, S., 2019. Heat-to-power conversion from variable surplus heat sources utilizing a thermal energy storage. Msc thesis, Norwegian University of Science and Technology

Schei, A., 1998. Production of high silicon alloys. Tapir, Trondheim, Norway.

Tangstad, M., 2013. Metal production in Norway. Akademika, Norway, 240.

Tveit, H., 1988. Størkning av 75% ferrosilisium : forløp, struktur og styrke. Ph.D. thesis, Norges Tekniske Høgskole, Trondheim.

Vance, D., Nimbalkar, S., Thekdi, A., Armstrong, K., Wenning, T., Cresko, J., Jin, M., 2019. Estimation of and barriers to waste heat recovery from harsh environments in industrial processes. Journal of Cleaner Production 222, 539 – 549.